Archives of Biochemistry and Biophysics 695 (2020) 108653

Contents lists available at ScienceDirect

Archives of Biochemistry and Biophysics

journal homepage: www.elsevier.com/locate/yabbi

Glycoproteomic analysis identifies cryptdin-related sequence 1 as *O*-glycosylated protein modified with α1,2-fucose in the small intestine

Hiroki Hashiguchi [a,b], Yohei Tsukamoto [a], Mitsutaka Ogawa [a,c], Yuko Tashima [a,c], Hideyuki Takeuchi [a,c], Masanao Nakamura [b], Hiroki Kawashima [b], Mitsuhiro Fujishiro [b], Tetsuya Okajima [a,c,*]

[a] Department of Molecular Biochemistry, Nagoya University Graduate School of Medicine, 65 Tsurumai-cho, Showa-ku, Nagoya, 466-8550, Aichi, Japan
[b] Department of Gastroenterology and Hepatology, Nagoya University Graduate School of Medicine, 65 Tsurumai-cho, Showa-ku, Nagoya, 466-8550, Aichi, Japan
[c] Institute for Glyco-core Research (iGCORE), Nagoya University, Furo-cho, Chikusa-ku, Nagoya, 464-8601, Japan

ARTICLE INFO

Keywords:
Cryptdin-related sequence 1
Defensin
Paneth cell
O-glycosylation
α1,2-fucose

ABSTRACT

The modification of galactose with α1,2-fucose is involved in symbiosis with intestinal bacteria and elimination of pathogenic bacteria. It is postulated that α1,2-fucosylated mucin secreted from goblet cells is involved in defending an organism against infections, but the detailed molecular mechanisms are yet to be elucidated. It was previously reported that Paneth cells of the small intestine were positive for UEA-1 lectin staining. However, glycoproteins in Paneth cells carrying α1,2-fucose have not yet been identified. Glycoproteomic analysis of ileal lysates identified 3212 O-linked and 2962 *N*-linked glycopeptides. In particular, cryptdin-related sequence 1 (CRS1) expressed in Paneth cells was found to be α1,2-fucosylated. Unlike other antimicrobial α-defensin proteins, CRS1 contains unique Thr residues, which are modified with O-glycans, with 3HexNAc2Hex1Fuc1NeuAc being the main glycoform. Identification of α1,2-fucose on the O-glycans of CRS1 expressed in Paneth cells will pave the way for a mechanistic understanding of α1,2-fucose-dependent symbiosis with intestinal bacteria and elimination of pathogenic bacteria in the intestine.

1. Introduction

Glycans play essential roles in cell-cell interactions [1]. The structures of these glycans are incredibly complex and diverse, and the interactions between glycans and glycan-recognizing molecules are closely related to the control of the development of organisms, and are involved in differentiation, proliferation, adhesion, gene expression, and signal transduction. Therefore, this knowledge can be applied to various fields, such as the diagnosis and treatment of diseases related to structural abnormalities in glycans [2].

The α1,2-linked fucose is a terminal structure that is commonly found in both *N*- and O-linked glycoproteins, the addition of which is catalyzed by members of the fucosyltransferase (FUT) family, i.e., FUT1 and FUT2 [3]. FUT1, formerly known as H enzyme, is primarily expressed in red blood cells in humans. It is involved in the formation of the H antigen, which is the precursor of the ABO blood group antigens [4,5]. In contrast, FUT2 is known as an Se enzyme in humans, where it is highly expressed in the epithelium of the digestive tract, including the oral cavity, stomach, small intestine, and large intestine [6]. Based on studies in various species, α1,2-fucosylation was shown to be involved in intestinal immunity [7]. In mice, α1,2-fucosylation of intestinal proteins by FUT2 activation serves as a carbon source for intestinal microorganisms, and plays an essential role in maintaining the normal microflora [8,9]. Furthermore, infections with *Salmonella typhimurium* are aggravated in the intestines of *Fut2*-deficient mice [10], and Std fimbriae of *S. typhimurium* interact with α1,2-fucose [11,12]. The aggravation of fungal infections with *Candida albicans* was shown in a similar mouse model [13]. Furthermore, the loss of FUT2-mediated α1,2-fucosylation

Abbreviations: CRS, cryptdin-related sequence; EIC, extracted ion chromatogram; Fuc, fucose; FUT, fucosyltransferase; Gal, galactose; GalNAc, N-acetylgalactosamine; GlcNAc, N-acetylglucosamine; HCD, higher energy collisional dissociation; IP-HILIC, ion-pair hydrophilic interaction liquid chromatography; LC-MS, liquid chromatography-mass spectrometry; NeuAc, N-acetylneuraminic acid; TCEP, tris (2-carboxyethyl) phosphine; TMT, tandem mass tag; UEA-1, *Ulex europaeus* agglutinin-1.

* Corresponding author. Department of Molecular Biochemistry, Nagoya University Graduate School of Medicine, 65 Tsurumai-cho, Showa-ku, Nagoya, 466-8550, Aichi, Japan.
E-mail address: tokajima@med.nagoya-u.ac.jp (T. Okajima).

https://doi.org/10.1016/j.abb.2020.108653
Received 22 September 2020; Received in revised form 22 October 2020; Accepted 24 October 2020
Available online 27 October 2020
0003-9861/© 2020 Elsevier Inc. All rights reserved.

impairs the binding of the adhesive factor BabA of *Helicobacter pylori* to the gastric mucosa [14].

Due to mutations in the *FUT2* gene, there are humans who cannot secrete H antigen into the saliva and gastric juices. The genotypes of secretion-competent individuals are *Se/Se* and *Se/se*, whereas that of secretion-defective individuals is *se/se*. The prevalence of the latter genotype is by no means rare, as exemplified by the fact that approximately 20% of the Danish population belongs to this group [15]. A person that is FUT2 secretion-defective due to a mutation in the *FUT2* gene is less likely to be infected with norovirus [16,17], but more at risk of developing chronic pancreatitis and stenoses in primary sclerosing cholangitis [18,19]. Furthermore, mutations in the *FUT2* gene have been suggested to be associated with type 1 diabetes [20], and to represent one of the causes of autoimmune inflammatory bowel diseases, including Crohn's disease [21,22]. In pigs, α1,2-FUT activity mediated by FUT1 is associated with the susceptibility of the small intestinal epithelium to *Escherichia coli* F18 adhesion [23].

The small intestine is an organ that is continuously in contact with a wide variety of symbionts of the bacterial flora and pathogenic microorganisms. However, various functions of α1,2-linked fucose in gut homeostasis remain unknown, and only a small number of glycoproteins have been reported to be α1,2-fucosylated. In this study, we aimed to determine novel α1,2-fucosylated glycoproteins related to intestinal homeostasis by analyzing endogenous intestinal glycoproteins through integrated proteomic analyses.

2. Materials and methods

2.1. Experimental animals

C57BL/6J mice were used in the course of this study. While being housed in an environment of 25 °C, the animals were allowed to consume solid feed and water, with light and dark periods alternating every 12 h. The experiments were conducted in accordance with the Animal Experimentation Rules of Nagoya University. All mice were subjected to cervical dislocation under sedation using isoflurane at 2–3 months of age, before undergoing midline laparotomy using scissors. For lipopolysaccharide (LPS) experiments, 10 μg of *S. typhimurium*-derived LPS (L6511, Sigma) per 1 g of mouse body weight were administered 24 h prior to necropsy by intraperitoneal injection.

2.2. Immunofluorescence staining of the mouse digestive tract

The stomach, as well as small and large intestines were collected and washed with phosphate-buffered saline (PBS). Small intestines were separated into three sections, corresponding to the duodenum, jejunum, and ileum. In this study, the duodenum was defined as the part of the small intestine located approximately 3 cm towards the anus from the gastric pylorus. The ileum was defined as the part of the small intestine located about 5 cm towards the mouth from the appendix. The middle part between these two sections was defined as the jejunum. After 16 h of fixation in 10 mL of 10% formalin in PBS, the tissues were soaked in an equal amount of PBS, followed by replacement by 10%, 20%, 30%, and 40% sucrose in PBS.

The samples were frozen in a 2-methylbutane solution that was cooled using liquid nitrogen. After removing the solvent, the samples were embedded in OCT compound (Tissue-Tek), and frozen using liquid nitrogen. The samples were sliced into 8 μm thick sections using a cryostat (CM3050S, Leica), attached to a slide glass, and dried to prepare sliced specimens. The latter were fixed with 4% paraformaldehyde in PBS for 15 min, followed by permeabilization with ice-cold 100% methanol for 5 min and 0.5% TritonX-100/PBS for 15 min.

For lectin staining, fixed samples were incubated with 5% fetal bovine serum (FBS) in PBS for 30 min, followed by biotinylated UEA-1 (Vector) diluted 100-fold in 5% FBS/PBS for 2 h, and Alexa Fluor Plus 488-conjugated streptavidin (Invitrogen) diluted 100-fold in 5% FBS/PBS for 2 h. Vectashield mounting medium with DAPI (Vector) was used as mounting agent. Stained samples were examined under an inverted fluorescence microscope (BZ-9000, Keyence).

2.3. Dissection of mouse intestines

Tubular small intestines were longitudinally opened into a flat sheet using micro-dissecting scissors. Any fecal matter, blood, and digestive fluids adhered to the inside of the intestines were removed using PBS. Approximately 5 mg of the tissue (1 mm in length) were lysed in 100 μL of 1 × Cell Lysis Buffer (Cell Signaling Technology) containing 1 mM phenylmethanesulfonyl fluoride (Funakoshi). The sample was centrifuged (4 °C, 4000×*g*, 20 min), and the supernatant was recovered. Debris was removed by passing through a 0.45 μm cellulose filter.

2.4. Plasmid construction

Expression vectors for wild-type and mutant forms of CRS1 (pcDNA3.1-CRS1:Myc-HisA and pcDNA3.1-CRS1Δ:Myc-HisA, respectively) were provided by GenScript. Full-length CRS1 cDNA was inserted into the pcDNA3.1 vector using *Hin*dIII and *Apa*I sites. T85V, T102V, T105V, T106V, and T111V mutations were introduced into the CRS1Δ expression vector.

2.5. Cell culture and transfections

Human embryonic kidney 293T (HEK293T) cells were cultured in high glucose (25 mM) DMEM (Sigma) supplemented with 10% FBS. Then, pcDNA3.1-CRS1:Myc-HisA and pcDNA3.1-CRS1Δ:Myc-HisA were transiently transfected into HEK293T cells using polyethylenimine (PEI Max, Polysciences), as described previously [24]. The cells were cultured in serum-free Opti-MEM medium (Thermo) after the transfection procedure.

Transfected cells and culture medium were recovered 72 h post-transfection. Cell lysates were prepared in TBS containing 1% TritonX-100 and a protease inhibitor cocktail (cOmplete Mini, EDTA-free, Sigma). For SDS-PAGE, samples were mixed with an equal volume of 2 × SDS sample buffer (40% glycerol, 4% SDS, 125 mM Tris-HCl, pH 6.8, 70 mM 2-mercaptoethanol, and 0.001% bromophenol blue), and the solution was boiled for 5 min at 90 °C. Each sample was separated by polyacrylamide gel electrophoresis with 17.5% running and 4.5% stacking gels [25]. After electrophoresis, the gel was stained for several hours using Coomassie dye (SimplyBlue Safe Stain, Invitrogen), placed into purified water, and shaken overnight in order to destain it.

2.6. Lectin and western blotting techniques

The transfer of proteins from polyacrylamide gels to PVDF membranes (Immobilon-P Transfer Membranes, Millipore) was performed using a semi-dry blotting device for 25 min at 25 V. After blocking with 5% bovine serum albumin (BSA) in PBS containing 0.05% Tween 20 for 30 min at room temperature (RT), the membrane was incubated at RT for 2 h with biotinylated UEA-1 (Vector) diluted 1000-fold in blocking solution, followed by HRP-labeled streptavidin (GE Healthcare) diluted 5000-fold in blocking solution for 1 h at RT. The membrane was incubated with Immobilon Western Chemiluminescent HRP Substrate (Millipore) prior to imaging. Signals were detected using the iBright CL1500 imaging system (Invitrogen). Western blotting with Myc-tag-specific antibody was performed as described previously [26].

2.7. Sample preparation by in-gel digestion

Excised polyacrylamide gel slices were soaked in 100 μL of acetonitrile for 10 min and dried using an evaporator. The solution was supplemented with 50 μL of 10 mM dithiothreitol/100 mM NH_4HCO_3 for 30 min at RT, followed by the addition of 50 μL of 50 mM

iodoacetamide/100 mM NH_4HCO_3 for 30 min at RT, 500 μL of 50% methanol/5% acetic acid for 16 h at 4 °C, and 200 μL of acetonitrile for 10 min. After drying using an evaporator, the gel was soaked in 50 μL of 25 mM NH_4HCO_3 containing 20 ng of trypsin (Sigma), and incubated for 16 h at 37 °C. The supernatant was desalinated using ZipTip C18 resin tips (Millipore), and dried using an evaporator.

2.8. Sample preparation by in-solution digestion

Approximately 10 mg of tissue samples were homogenized in 500 μL of lysis buffer (1% SDS, 10 mM TCEP, 40 mM 2-chloroacetamide, and 50 mM NH_4HCO_3). The homogenate was boiled for 15 min at 90 °C, and centrifuged at 1000×*g* for 10 min. The supernatant was collected and mixed with 50 μg of trypsin (Sigma) dissolved in 10 μL of 0.01% trifluoroacetic acid. The mixture was incubated for 16 h at 37 °C, and boiled for 30 min at 90 °C. Then, SDS was precipitated by adding 500 μL of 1% trifluoroacetic acid. The supernatant was recovered and passed through a 0.45 μm cellulose filter. The filtrate was desalinated using a Sep-Pak C18 column (Waters) and dried using an evaporator.

2.9. Tandem mass tag (TMT) labeling and α1,2-fucosidase treatment

The combined glycopeptides enriched by ion-pair hydrophilic interaction liquid chromatography (IP-HILIC) were dissolved in 50 μL of triethylammoniumbicarbonate and split into two aliquots. Using TMT 2-plex (Thermo) by following the manufacturer's protocol, the two samples were labeled with TMT2-126 and TMT2-127, respectively, desalinated using ZipTip C18 resin tips, and dried using an evaporator. Dried samples were dissolved in 10 μL of 1 × GlycoBuffer (NEB). TMT2-127-labeled peptides were treated with 1 μL of α1,2-fucosidase (NEB), whereas TMT2-126-labeled peptides remained untreated. After 16 h, the two samples were mixed, desalinated using a ZipTip C18 resin tip, and dried using an evaporator.

2.10. IP-HILIC

The samples were dissolved in 80% acetonitrile/0.1% trifluoroacetic acid and subjected to HPLC (CBM-20A Series, Shimadzu) equipped with an Amide-80 column (dimensions of 4.6 × 250 mm and a particle size of 5 μm, TSKgel). After sample loading, the column hydrophilicity was increased by employing a linear gradient ranging from 80% acetonitrile/0.1% trifluoroacetic acid to 40% acetonitrile/0.1% trifluoroacetic acid over the course of 30 min. A total of 30 fractions were collected, and fractions 18 to 25 were mixed and dried using an evaporator.

2.11. Affinity purification using UEA-1

Agarose-bound UEA-1 (Vector) equilibrated in PBS was mixed with the tryptic digests and incubated at 4 °C for 2 h. After three sequential washes with PBS, bound peptides were eluted with 0.1 M glycine-HCl, pH 2.7. The eluate was mixed with 1 M Tris-HCl, pH 9.0, to neutralize the sample. The latter was then desalinated using a ZipTip C18 resin tip and dried with an evaporator.

2.12. Liquid chromatograpy-mass spectrometry (LC-MS)/MS analysis

Samples were dissolved in 20% acetonitrile/0.1% trifluoroacetic acid. The mass spectrometer used was a Q Exactive (Thermo), which was connected to an UltiMate 3000 RSLCnano System (Thermo). The liquid chromatography column used was a Nano HPLC capillary column at 150 mm × 75 μm (Nikkyo Technos). Reverse-phased liquid chromatography was run at a flow rate of 300 nL/min. The linear gradient profile ranged from 20% acetonitrile/0.1% trifluoroacetic acid to 80% acetonitrile/0.1% trifluoroacetic acid, and was run over 45 min. Electrospray ionization was used as ion source. The analytical parameters used were positive ion mode, a resolution of 140,000, an acquisition range of 400 to 1600 *m/z*, and MS1 full scan at an automatic gain control of 1.0×10^6. The 10 most intense precursor ions were selected for higher energy collisional dissociation (HCD) MS/MS fragmentation. The collision energy was set to a stepped normalized collision energy of 15/25/35. The analytical conditions were an automatic gain control of 1.0×10^5, an isolation window of 2.0, dynamic exclusion of 15 s, fragment resolution of 17,500, and measured ion valence of 2–5. Both MS1 and MS2 spectra were acquired with a mass accuracy of 10 ppm using Orbitrap.

In the spectral data analysis of glycopeptides, the obtained raw data were processed by Byonic (MS1 tolerance: 10 ppm, MS2 tolerance: 20 ppm) as a node for Proteome Discoverer 2.3 (Thermo). *Mus musculus* (SwissProt 10,090) was specified as the species the protein database of which was to be searched. The glycan list included 309 and 78 mammalian *N*- and O-glycans, respectively, based on the standard settings for Byonic. Other search parameters were as follows: carbamidomethylation of cysteine residues as fixed modifications, and oxidation of methionine residues as variable modifications. The analysis was performed using a false discovery rate (FDR) of 0.01. For qualitative analyses, we detected the b/y ions and glycan-derived fragment ions in the MS2 spectrum using the Xcalibur Qual browser (Thermo). Semi-quantitative analysis was performed using the relative height of the extracted ion chromatogram (EIC) of the most abundant isotope peak of the precursor ion using the Xcalibur Quan browser (Thermo).

2.13. Data availability

Glycoproteomics data are available by accessing JPOST at the following URL: https://repository.jpostdb.org/

ID: JPST000988

3. Results

3.1. Distribution of α1,2-fucosylated proteins in the mouse digestive tract

In order to detect the distribution of α1,2-fucosylated proteins in the mouse digestive tract (Fig. 1A), we performed lectin staining with UEA-1, which specifically recognizes α1,2-linked fucose. Fluorescent staining showed a positive signal at the mucosal surface in the stomach, small intestines (duodenum, jejunum, and ileum), and large intestines (Fig. 1B). In the jejunum and ileum, additional signals were observed in Paneth cells. As shown in the magnified image, vesicle-associated granules inside the Paneth cells were heavily stained. These results suggest that glycoproteins modified by α1,2-fucosylation are abundant in Paneth cells of healthy mice with normal bacterial flora. However, when the mice were culled after intraperitoneal administration *of S. typhimurium*-derived LPS according to the intestinal bacterial infection stimulation model [10], intense staining of the mucin layer of the ileal epithelium was observed, but no changes were observed in Paneth cell staining patterns.

Next, lysates from each tissue were subjected to UEA-1 lectin blotting to detect α1,2-fucosylated proteins. Strong signals in the jejunum and ileum with an apparent molecular weight of 15 kDa were observed in addition to high molecular weight species (Fig. 1C). The broad smear-like band suggested the existence of glycosylation.

3.2. Glycoproteomics of the mouse ileum identifies cryptdin-related sequence 1 (CRS1) as an O-linked glycopeptide

In order to identify novel α1,2-fucosylated glycoproteins in the mouse ileum, we performed a comprehensive glycoproteomic analysis. Samples were prepared from mouse ileal lysates by in-solution digestion, followed by glycopeptide enrichment by IP-HILIC (Fig. 2A), and obtained mass spectral data were analyzed using Proteome Discoverer and Byonic (Fig. 2B). By counting the highly reliable peptides matching

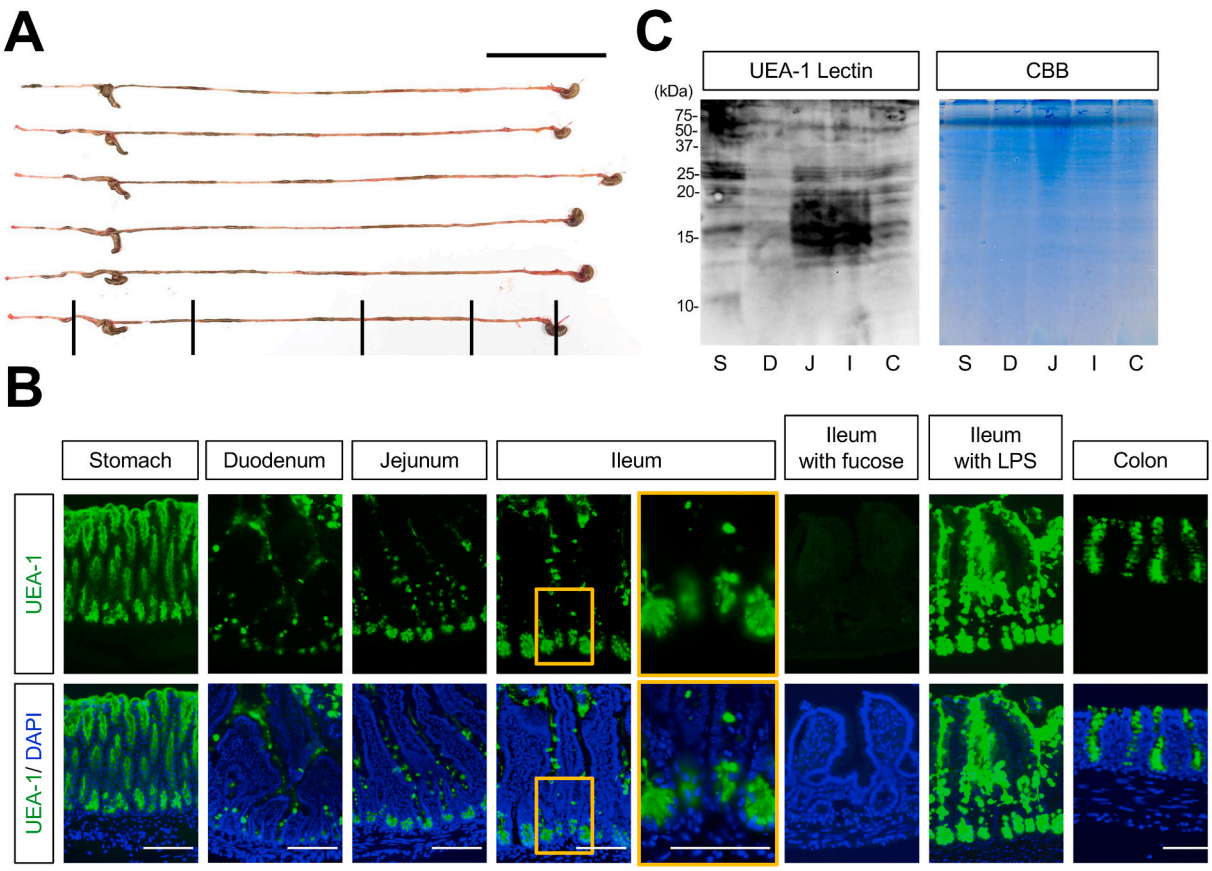

Fig. 1. α1,2-fucosylated glycoproteins are abundantly expressed in Paneth cells in the small intestine. (A) Dissected mouse gastrointestinal tracts. Scale bar, 10 cm; the proximal part is shown on the right. (B) UEA-1 lectin staining. Scale bar, 100 μm. Blue, DAPI; green, Alexa 488 coupled to UEA1. The top row indicates UEA-1 staining, and merged images are shown in the bottom panel. In the stomach and colon, the mucosal surface was stained with UEA-1. In contrast, the jejunum and ileum show additional staining in Paneth cells. A magnified image of the boxed region in the ileum is shown on the right. Treatment with LPS markedly increased the signal at the mucosal surface in small intestines, but not in Paneth cells. (C) Coomassie Brilliant Blue (CBB) staining and lectin blots of lysates from the gastrointestinal tracts. S, stomach; D, duodenum; J, jejunum; I, ileum; C, colon. (For interpretation of the references to colour in this figure legend, the reader is referred to the Web version of this article.)

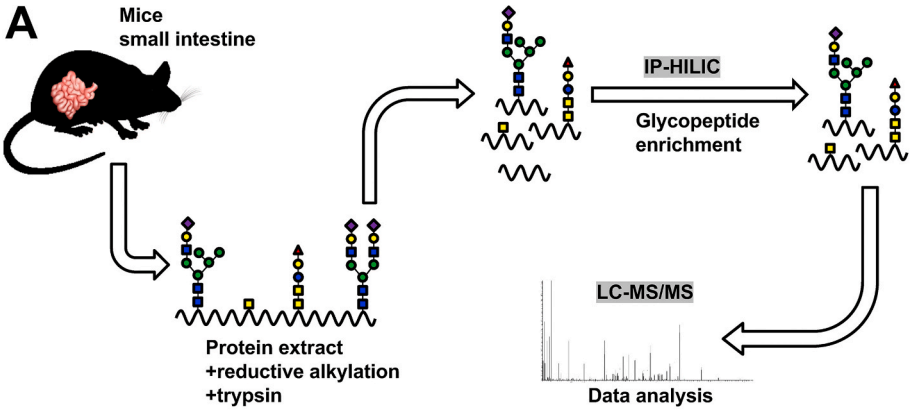

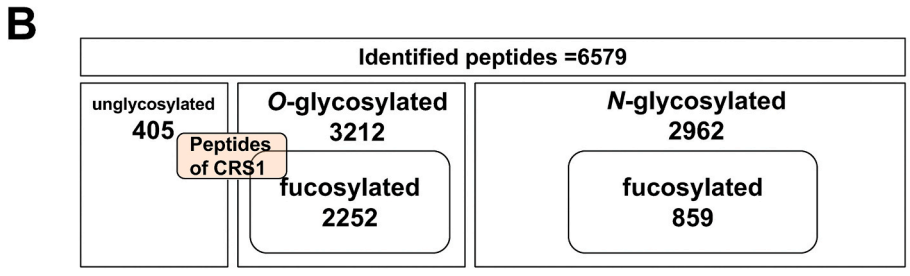

Fig. 2. Mass spectrometric analysis of mouse ileal lysates. (A) Schematic of the experimental procedures. Mouse ileal lysates were reduced, alkylated, and trypsin-digested. The enrichment of glycopeptides was then performed by IP-HILIC, followed by analysis by LC-MS/MS. (B) Classification of peptides identified by LC-MS/MS analysis. Out of the 6579 peptides identified, 405 were unglycosylated, 3212 were modified with O-glycans (2252 of which contained fucose), and 2962 were modified with *N*-glycans (859 of which included fucose).

an FDR <0.01 using Byonic, we identified 6579 peptides. These included 405 unglycosylated peptides, 3212 O-linked glycopeptides (out of which 2252 contained fucose), and 2962 *N*-linked glycopeptides (out of which 859 contained fucose). The O-linked and *N*-linked glycopeptides correspond to 1220 and 565 glycoproteins, respectively (Table S1). In addition to the major intestinal glycoproteins of mucin, which is assumed to act as an infection barrier (Fig. S1), a large number of glycopeptides derived from CRS1 (UniProt ID: P17533.2; GenBank ID: AK008584.1), a putative antimicrobial peptide, were identified. CRS1 (also called α-defensin 29) is expressed in Paneth cells in the intestine [27]. These results suggested that CRS1 is a fucosylated protein in mouse ileal Paneth cells.

The amino acid sequence of CRS1 was partially homologous to that of α-defensins 1 and 2, which are representative proteins of the α-defensin family (Fig. 3A and Fig. S2). As expected from the processing of the pro-domain, two CRS1 peptides, CPVCPTCPQCPK and TAITTQAPNTQHK, were located at the *C*-terminal mature domain. There were 5 and 30 types of O-linked glycoforms observed for CPVCPTCPQCPK and TAITTQAPNTQHK, respectively, thus constituting a large proportion of the 348 O-linked glycopeptides identified. CPVCPTCPQCPK contains only a single modification site that is modified with multiple forms of O-glycans, with 3HexNAc2Hex1Fuc1NeuAc being the most abundant glycoform (Fig. 3B). Although TAITTQAPNTQHK contains multiple modifiable sites that make it nearly impossible to assign the actual glycosylation sites, the 3HexNAc2Hex1Fuc1NeuAc glycan similarly represented the major glycoform (Fig. 3B). These results indicate that CRS1 is modified with fucose-containing O-glycans.

Previous glycomic analyses demonstrated that core 2-type O-glycans were the dominant forms in the mouse small intestine, and, among those, the 3HexNAc2Hex1Fuc1NeuAc glycoform contained the Sd^a epitope (GalNAc-β1,4 [NeuAc-α2,3]Gal) and H antigen (Fuc-α1,2Gal) [28]. However, the proteins carrying this type of glycan have not yet been identified. To determine whether CRS1 O-glycans are modified with fucose via α1,2-linkage, MS-based quantification using a TMT was performed on mouse ileal lysates. The TAITTQAPNTQHK glycopeptide with 3HexNAc2Hex1Fuc1NeuAc was markedly decreased after enzymatic digestion with α1,2-fucosidase, whereas 3HexNAc2Hex1NeuAc, a predicted digestion product, was increased (Fig. 3C). These results demonstrated the α1,2-fucosylation of CRS1.

To determine the detailed glycan structures on CRS1, fragment ions of glycopeptides enriched by IP-HILIC were analyzed (Fig. 4 and Fig. S3). Fragment ions lacking non-reducing terminal fucose, NeuAc, and HexNAc, in addition to those featuring core 2-type O-glycans, were successfully assigned to CPVCPTCPQCPK glycopeptides (Fig. 4A). These data are consistent with the predicted glycan structure containing the Sd^a epitope and H antigen [28]. A small amount of the same peptide without O-glycosylation was also detected (Fig. 4B). A similar MS/MS profile indicative of the presence of core 2-type O-glycans was obtained for TAITTQAPNTQHK glycopeptides, although O-glycosylation possibly occurred on multiple sites instead of a single site (Fig. 4C). However, the presence of an unglycosylated form of the peptide (Fig. 4D) indicated that the *O*-GalNAc modification of this peptide was substoichiometric, and thus the population of glycopeptides carrying multiple O-glycans, such as the 6HexNAc4Hex2NeuAc glycoform (Fig. 3B), were minor forms, at least in the ileum. Nonetheless, these results demonstrated that CRS1 contains one or more core 2-type O-glycans with α1,2-linked fucose.

To further confirm the α1,2-fucosylation of CRS1, we performed

A

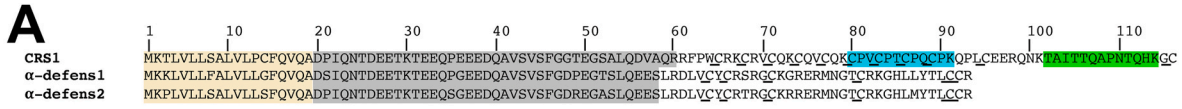

B

^{80}CPVCPTCPQCPK^{91}	
Glycoform	**Relative abundance**
HexNAc(3)Hex(2)Fuc(1)NeuAc(1)	3.91E^7
HexNAc(2)Hex(2)Fuc(1)NeuAc(1)	2.42E^7
HexNAc(3)Hex(2)NeuAc(1)	1.61E^7
HexNAc(2)Hex(1)NeuAc(2)	5.26E^6
HexNAc(3)Hex(3)NeuAc(1)	3.32E^6

^{102}TAITTQAPNTQHK^{114}	
Glycoform	**Relative abundance**
HexNAc(3)Hex(2)Fuc(1)NeuAc(1)	5.08E^8
HexNAc(3)Hex(2)NeuAc(1)	2.39E^8
HexNAc(2)Hex(2)NeuAc(1)	1.83E^8
HexNAc(2)Hex(2)Fuc(1)NeuAc(1)	1.60E^8
HexNAc(3)Hex(3)NeuAc(1)	9.49E^7
HexNAc(2)Hex(2)NeuAc(2)	6.49E^7
HexNAc(3)Hex(2)Fuc(1)	5.67E^7
HexNAc(3)Hex(2)Fuc(2)NeuAc(1)	4.34E^7
HexNAc(2)Hex(1)Fuc(2)	3.46E^7
HexNAc(3)Hex(3)Fuc(2)	3.34E^7
HexNAc(2)Hex(1)NeuAc(1)	2.68E^7
HexNAc(3)Hex(2)Fuc(3)	2.68E^7
HexNAc(2)Hex(2)	2.42E^7
HexNAc(4)Hex(4)Fuc(2)	2.29E^7
HexNAc(3)Hex(2)NeuAc(2)	2.10E^7
HexNAc(3)Hex(2)NeuAc(1)	1.86E^7
HexNAc(4)Hex(5)Fuc(3)	1.81E^7
HexNAc(2)Hex(2)Fuc(1)	1.39E^7
HexNAc(6)Hex(4)NeuAc(3)	1.28E^7
HexNAc(4)Hex(2)NeuAc(1)	1.05E^7
HexNAc(6)Hex(4)NeuAc(3)	1.00E^7
HexNAc(4)Hex(4)	8.64E^6
HexNAc(4)Hex(4)Fuc(3)	8.42E^6
HexNAc(5)Hex(4)Fuc(3)	7.29E^6
HexNAc(6)Hex(4)Fuc(2)NeuAc(2)	7.15E^6
HexNAc(2)Hex(1)NeuAc(2)	7.06E^6
HexNAc(5)Hex(4)Fuc(3)	5.47E^6
HexNAc(3)Hex(1)NeuAc(1)	5.24E^6
HexNAc(4)Hex(2)NeuAc(2)	4.55E^6
HexNAc(4)Hex(3)NeuAc(1)	4.34E^6

C

^{102}TAITTQAPNTQHK^{114}		
Glycoform	**HexNAc(3)Hex(2)Fuc(1)NeuAc(1)**	**HexNAc(3)Hex(2)NeuAc(1)**
Control	168.9	31.1
α1,2-fucosidase	61.8	138.2
α1,2-fucosidase/Control	0.184	2.238

Fig. 3. Cryptdin-related sequence 1 (CRS1) is *O*-glycosylated and contains α1,2-linked fucose. (A) Amino acid sequence alignment of CRS1, α-defensin 1 (α-defens1), and α-defensin 2 (α-defens2). CPVCPTCPQCPK and TAITTQAPNTQHK peptides were modified with fucose-containing O-glycans. Yellow and gray highlights indicate signal peptides and pro-peptides, respectively. (B) Lists of O-glycans detected on the indicated CRS1 peptides. Relative abundances are also shown. (C) Digestion of the TAITTQAPNTQHK peptide with α1,2-fucosidase. The glycoform of 3HexNAc2Hex1Fuc1NeuAc was decreased after digestion, whereas that of 3HexNAc2Hex1Sia was increased. (For interpretation of the references to colour in this figure legend, the reader is referred to the Web version of this article.)

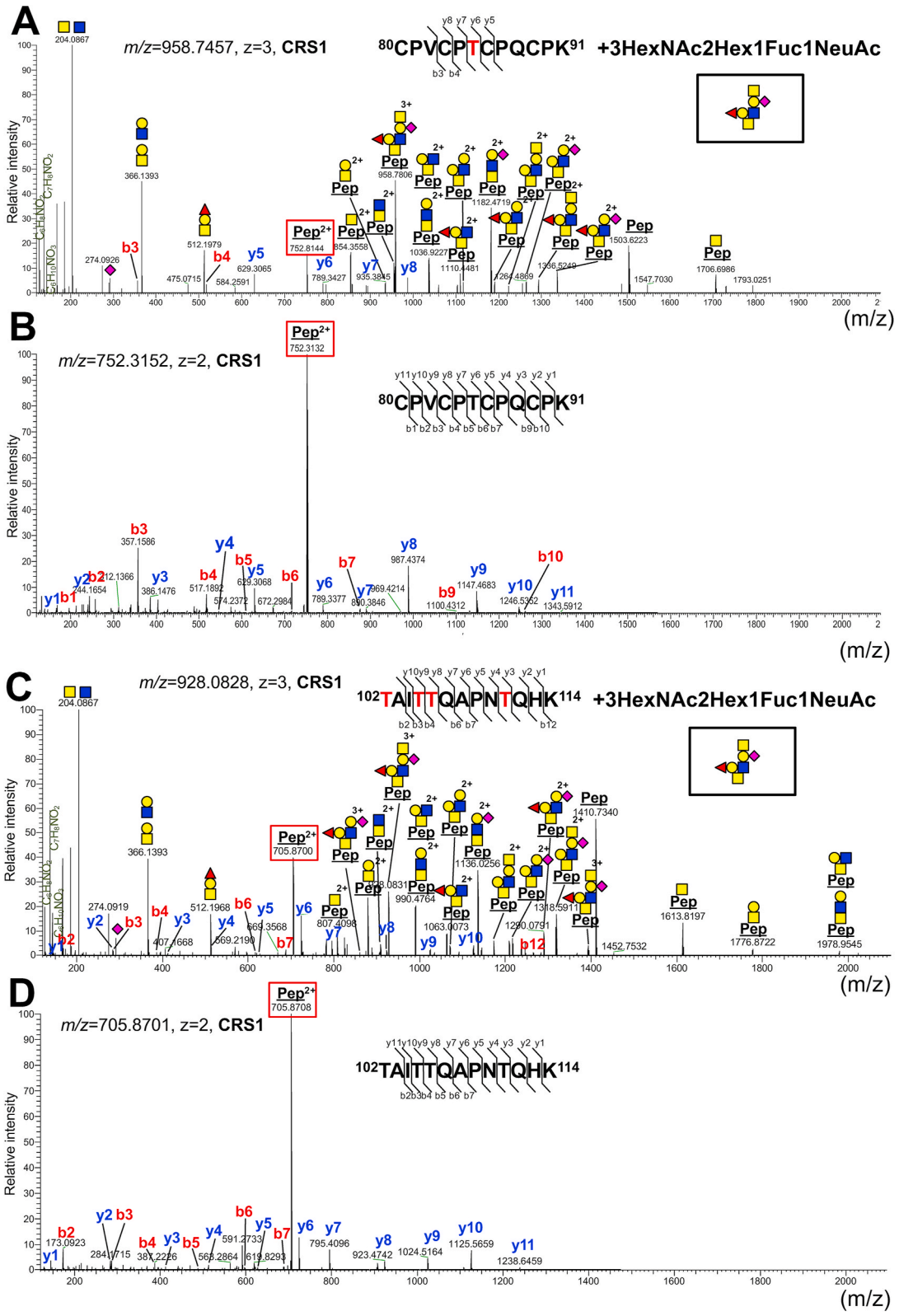

Fig. 4. MS/MS profiles of glycopeptides from CRS1. (A) MS/MS spectra of CPVCPTCPQCPK glycopeptides with 3HexNAc2Hex1Fuc1NeuAc. The observed fragment ions are consistent with the presence of the indicated core 2-type O-glycans. (B) MS/MS spectra of the CPVCPTCPQCPK peptide without glycosylation. The vertical axis indicates relative abundance, and the horizontal axis indicates *m/z*. (C) MS/MS spectra of TAITTQAPNTQHK glycopeptides with 3HexNAc2Hex1Fuc1NeuAc. Red and blue letters represent b and y ions, respectively. The observed fragment ions are consistent with the presence of the indicated core 2-type O-glycans, although modifications on multiple sites cannot be excluded. (D) MS/MS spectra of TAITTQAPNTQHK peptides not modified by O-glycans. (For interpretation of the references to colour in this figure legend, the reader is referred to the Web version of this article.)

affinity precipitation of glycopeptides from mouse ileal lysates using UEA-1 lectin-coated agarose beads. Subsequent glycoproteomic analysis led to the identification of the TAITTQAPNTQHK peptide modified by 3HexNAc2Hex1Fuc1NeuAc, further suggesting α1,2-linked fucosylation of CRS1 (data not shown).

3.3. CRS1, but none of the other α-defensins, is O-glycosylated

To analyze the differential glycosylation patterns between CRS1 and other α-defensin proteins, we performed MS analysis using in-gel digestion. UEA-1 lectin blotting of mouse ileal lysates showed a positive signal at a molecular weight of ~15 kDa (Fig. 5A). Other α-defensins with a molecular weight of 10 kDa appeared to be negative for UEA-1 staining and served as negative controls. Lysates were separated by SDS-PAGE, and the excised gel fragments containing glycosylated CRS1 or α-defensin proteins were subjected to in-gel digestion and mass spectrometric analysis (Fig. 5B). In the control samples, 11 types of bactericidal proteins, including α-defensins 1, 2, 5, 8, 9, 15, 16, 20, 21, 22, 23, 24, and 26, were identified as unglycosylated peptides (Fig. S2). Glycopeptides derived from these proteins were not identified. In contrast, mass spectrometric analysis of the UEA-1-positive region identified TAITTQAPNTQHK glycopeptides from CRS1 in addition to the unglycosylated peptide. These results suggested that CRS1, but none of the other α-defensins, was modified with O-glycans and α1,2-linked fucose.

To exclude the possibility that decreased ionization efficiencies precluded the detection of glycopeptides, unglycosylated peptides were removed by the IP-HILIC technique (Fig. 5C). As expected, glycopeptides enriched from the UEA-1-positive region led to the detection of TAITTQAPNTQHK glycopeptides modified with O-glycans (Fig. 5C and D), but not of unglycosylated peptides. In contrast, no α-defensin peptides were identified from either the UEA-1-positive or control regions. These results revealed that glycopeptides of 15 kDa that were detectable by UAE-1 lectin staining included CRS1 modified with O-glycans containing α1,2-linked fucose.

3.4. O-glycans are dispensable for the dimerization of CRS1

It has been shown that the α-defensin family of antimicrobial peptides forms dimers or higher-order aggregates that are linked to the molecular mechanisms underlying membrane permeabilization of microbes [32]. To determine whether O-glycans are required for dimer formation of CRS1, a mutant form of CRS1 lacking five putative O-glycosylation sites (CRS1Δ, Fig. 6A) was generated. Expression of CRS1 or CRS1Δ in HEK293T cells revealed dimer formation of CRS1 in the culture media irrespective of the presence of glycans. These data indicated that O-glycans were dispensable for dimer formation of CRS1 (Fig. 6B).

4. Discussion

We carried out a comprehensive glycoproteomic analysis of glycosylated proteins in the mouse small intestine. Studies in humans and mice have shown that α1,2-fucosylation of proteins present in the small intestinal epithelium plays a major role in maintaining normal microflora balance, as well as for eliminating pathogenic bacteria [29]. According to the latest research, the expression of FUT2 in intestinal epithelial cells can be increased by host stimulation through the administration of *Salmonella*-derived LPS, resulting in increased intensity of UEA-1 staining, primarily on the surface of the small intestines [10]. While supporting these reports, our study noted no changes in the intensity of UEA-1 staining after LPS stimulation of Paneth cells, thus indicating that the expression of α1,2-fucosylated proteins was constitutive (Fig. 1B). Microarray analysis showed that FUT1 and FUT2 were expressed in Paneth cells [30], which was consistent with the positive UAE-1 lectin staining in *Fut2* mutant mice [10].

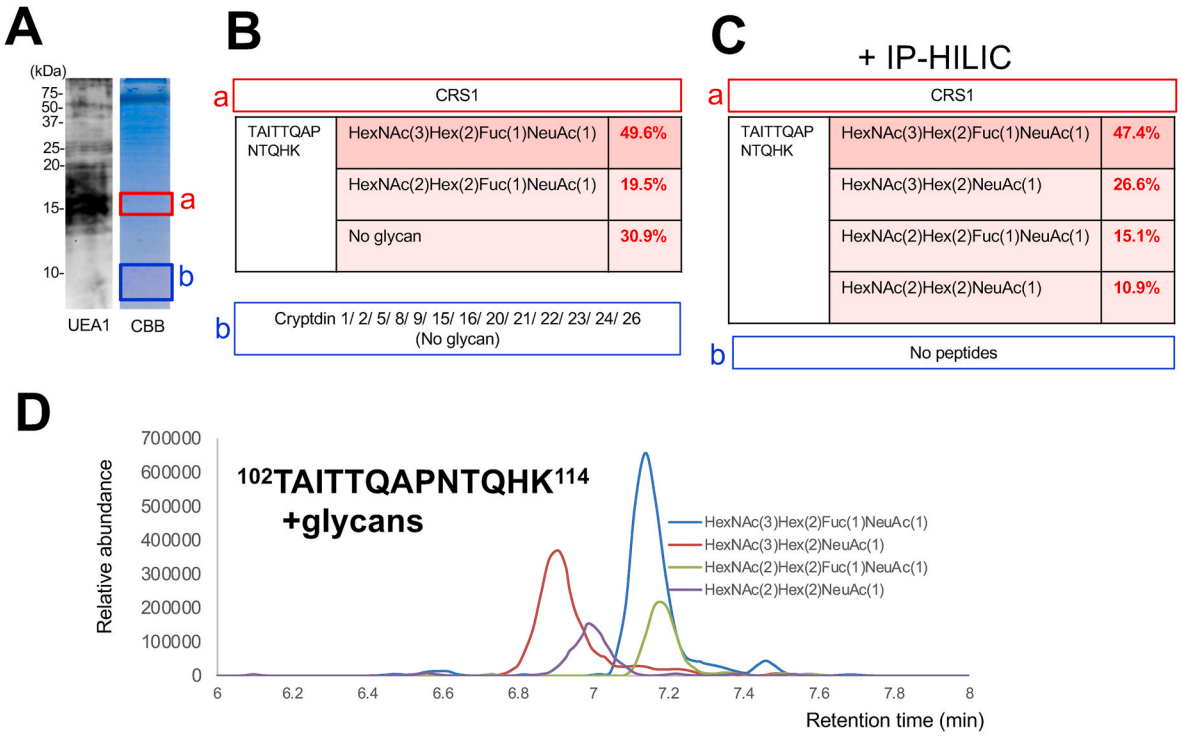

Fig. 5. CRS1, but none of the other α-defensin proteins, is *O*-glycosylated. (A) Lectin blotting indicating the area of the gels excised for mass spectrometric analysis. UEA-1-positive and -negative areas (at around 15 and 10 kDa, respectively) are marked by boxes. (B) CRS1 glycopeptides were identified from the UEA-1-positive area. In samples derived from the UEA-1-negative region, CRS1 was not detected, whereas 11 α-defensin family proteins were identified. (C) Enrichment of glycopeptides by IP-HILIC increased the number of detectable glycoforms on CRS1. No glycans were detected on other α-defensin proteins. (D) Semi-quantitative analysis of CRS1 glycoforms based on extracted ion chromatogram (EIC) of precursor ions.

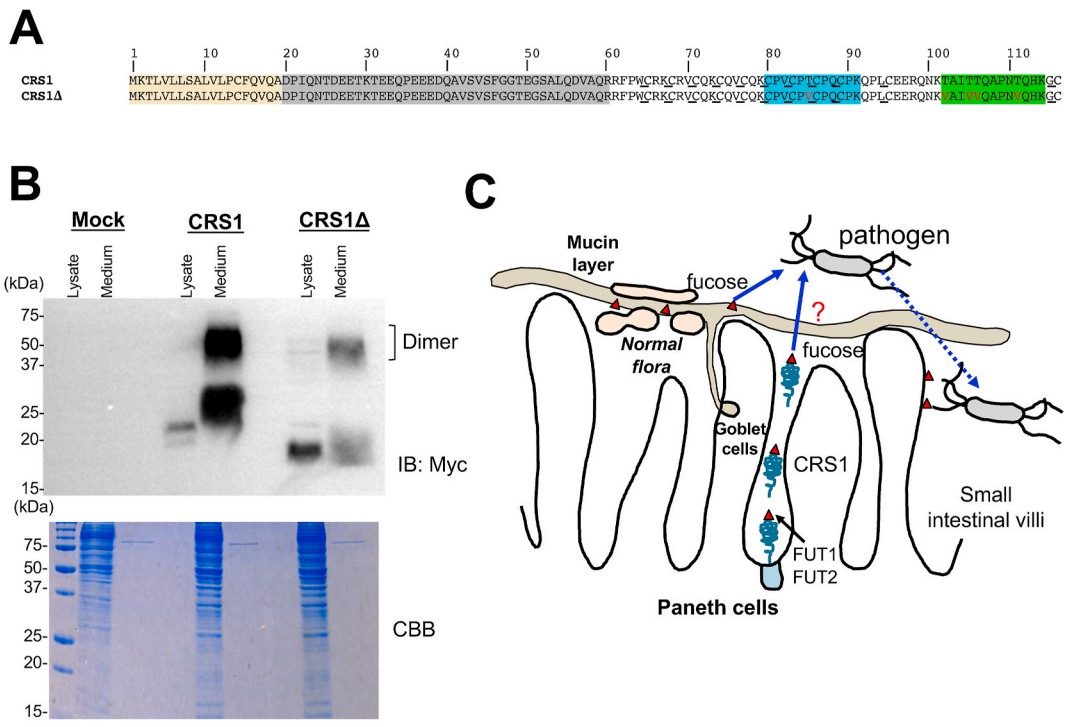

Fig. 6. O-glycans on CRS1 are dispensable for the dimerization of CRS1. (A) Amino acid sequences of CRS1 and the glycosylation mutant lacking five potential O-glycosylation sites. (B) Immunoblotting of cell lysates and culture media prepared from HEK293T cells expressing CRS1 or the CRS1 mutant (CRS1Δ). Detection with *anti*-Myc antibody revealed that the dimerization of CRS1 was not affected by loss of glycosylation. Coomassie Brilliant Blue (CBB) staining shows similar protein loading. (C) Model showing the potential physiological function of α1,2-fucosylated CRS1. Fucosylated molecules in the intestinal epithelium interact with Std fimbriae of *S. typhimurium,* thus contributing to the infection process. Mucin secreted by goblet cells contains α1,2-linked fucose, and, therefore, is assumed to protect from infections with pathogens. The presence of α1,2-fucose on CRS1 may facilitate the interaction with pathogens, although the physiological functions of CRS1 await future studies. (For interpretation of the references to colour in this figure legend, the reader is referred to the Web version of this article.)

In the present study, MS analysis showed that CRS1 undergoes O-glycosylation, which includes α1,2-fucosylation. In addition, quantitative analysis using EIC showed that the 3HexNAc2Hex1Fuc1Sia glycan was the most abundant glycoform. In contrast, many α-defensin family proteins other than CRS1 were found not to be glycosylated.

Defensins are typical mammalian cationic bactericidal peptides and major factors in innate immunity [31]. Among them, the synthesis of α-defensins is limited to Paneth cells in the small intestine. Paneth cells respond to bacterial and cholinergic stimuli and rapidly secrete α-defensin-containing granules into the lumen of the small intestine. Secreted α-defensin binds to the bacterial cell membrane and attacks bacteria by opening up holes in the membrane [32]. As a specific example of α-defensin activation, cryptdin 1 (mouse α-defensin 1) exists as pro-cryptdin 1 in vesicular granules of Paneth cells, and is converted to activated cryptdin 1 through cleavage of the pro-peptide by matrilysin (matrix metalloproteinase-7, MMP-7) [33]. Mice lacking activated cryptdin 1 reportedly have a small intestinal flora significantly different from that of wild-type mice [32]. While cryptdin 1 exerts strong bactericidal activity against pathogenic bacteria, it has no bactericidal activity against the constituents of the normal bacterial flora, such as *Lactobacillus*, *Bifidobacterium*, and *Bacteroides* [34]. This suggests that the α-defensin family of proteins secreted by Paneth cells elicits their bactericidal effects to control the composition of intestinal bacteria and maintain the homeostasis of a healthy microflora [35]. A study in mice showed that changes to the intestinal microflora, where specific cryptdin deficiencies lead to an increase in specific bacterial species, are clinically associated with Crohn's disease, obesity, graft-versus-host disease, and protozoal infections [21,22].

The gene encoding mouse α-defensin consists of two exonic regions on mouse chromosome 8 [36,37], and the mouse α-defensin family is a very diverse group of proteins that are largely classified into α-defensins 1 to 43 and α-defensin-related sequences 1 to 12. There are those who target gram-positive and gram-negative bacteria, including the normal bacterial flora [38]. Structurally, all types of α-defensins, 10 kDa proteins consisting of 91–93 amino acid residues, have a conserved structure containing three disulfide bonds in the active site, and are also comparable in terms of the signal peptides and pro-domain sequences at the *N*-terminus. Compared with the α-defensin family of proteins, CRS proteins have unique characteristics, such as different positions of cysteines putatively forming disulfide bonds in the matured protein domain. CRS proteins are unique in mice, and are encoded by a gene on chromosome 8, a locus contiguous with that of α-defensin [39]. Although only few studies focusing specifically on CRS1 have been conducted thus far, a report on the antimicrobial effect of CRS4 in mice [40] supports the idea that CRS proteins are functionally similar to α-defensin proteins.

Compared with α-defensin proteins, CRS1 contains 20 additional amino acid residues at the *C*-terminus, which results in a total of 116 amino acids and a heavier molecular weight of 15 kDa (Fig. 5A). In the vicinity of the *C*-terminus, the CPVCPTCPQCPK and TAITTQAPNTQHK peptides both had potential O-glycosylation sites, where GalNAc was attached to Ser/Thr residues. A variety of glycoforms was found for both peptides, with the most frequently observed pattern being 3HexNAc2Hex1Fuc1NeuAc, which corresponded to previously identified glycans featuring an Sd^a epitope and H antigen [28].

In addition to CRS1, we identified 11 other types of α-defensin family proteins in the mouse small intestine, namely α-defensins 1, 2, 5, 8, 9, 15, 16, 20, 21, 22, 23, 24, and 26. The peptides were identified as unglycosylated peptides; no glycans were detected, regardless of the enrichment of glycoproteins. Based on these results, the additional *C*-terminal sequence characteristic of CRS1 is critical for O-glycosylation.

Glycans impart various effects and functions to the modified protein. Although CRS1 constitutes one of the glycoproteins modified with α1,2-fucose in Paneth cell granules, the molecular functions, including the

antimicrobial activity, await further research. Previous research has revealed that stimulation of the host gut environment with infectious agents leads to the activation of glycosyltransferases, including FUT2. However, CRS1 appears to be constitutively α1,2-fucosylated by the combined actions of FUT1 and FUT2.

Symbiotic and antibiotic interactions between the gut microbiota and the host are complex processes, where α1,2-fucose exerts pleiotropic effects. The results of this study added a new player that could act through a novel molecular mechanism. Unfortunately, because the molecular functions and targets of CRS1 remain unknown, we must await future studies aiming to analyze the effect of α1,2-fucosylation on CRS1 activity. It should be noted, however, that our findings on CRS1 with α1,2-fucosylation provide the first example of a member of the α-defensin family of peptides that is modified with O-glycans and α1,2-fucose. If these modifications turn out to impact the antimicrobial activity of CRS1, this will invoke a new concept of "antimicrobial glycopeptides". Recent research suggests that Std fimbriae of *S. typhimurium* bind to α1,2-fucose, and that they are essential for colonization of the intestinal tract [11,12]. It has also been speculated that mucin modified with α1,2-fucose secreted by goblet cells could trap *Salmonella*. Notably, most of the CRS1 proteins in the ileum are α1,2-fucosylated regardless of LPS administration (data not shown). Based on these findings, it is tempting to speculate that the α1,2-fucose moiety on CRS1 functions to target microbes that interact with α1,2-fucose to elicit protein activities without an immune response (Fig. 6C).

Understanding the function of Paneth cells in the small intestine leads to an understanding of the mechanisms employed to maintain intestinal homeostasis, as well as of the pathogenesis of intestinal tract-related diseases accompanying the collapse of the intestinal flora, thus paving the way for the development of prophylactic and therapeutic approaches. Demonstration of α1,2-fucosylation of CRS1 will deepen our knowledge of Paneth cells in intestinal homeostasis.

Author contributions

HH designed the entire project. HH and YoT carried out cell biological and animal studies, and analyzed the data. MO assisted in mass analysis. YuT and HT supported the sample preparation and analysis. MN, HK, and MF assisted in cell biological and histological studies. HH prepared the manuscript. TO procured the research funds and supervised the research.

Declaration of competing interest

The authors declare no conflicts of interest.

Acknowledgments

We thank K. Taki (Nagoya Univ) for performing the LC-MS/MS analyses, N. Toida (Nagoya Univ) for technical support, and K. Furukawa (Chubu Univ) for supervising and supporting the project. This work was supported by JSPS KAKENHI Grant Numbers JP19H03416 (to TO) JP19H03176 (to HT), 19KK0195 (to HT), and JP19K16073 (to MO), as well as by grants from the Mitsubishi Foundation (to TO), the Japan Foundation for Applied Enzymology (to TO), the Takeda Science Foundation (to MO), and the Foundation for Promotion of Cancer Research in Japan (to MO).

Appendix A. Supplementary data

Supplementary data related to this article can be found at https://doi.org/10.1016/j.abb.2020.108653.

References

[1] K. Ohtsubo, J.D. Marth, Glycosylation in cellular mechanisms of health and disease, Cell 126 (5) (2006) 855–867.
[2] K.W. Moremen, M. Tiemeyer, A.V. Nairn, Vertebrate protein glycosylation: diversity, synthesis and function, Nat. Rev. Mol. Cell Biol. 13 (7) (2012) 448–462.
[3] D.J. Becker, J.B. Lowe, Fucose: biosynthesis and biological function in mammals, Glycobiology 13 (7) (2003) 41r–53r.
[4] N.D. Avent, Human erythrocyte antigen expression: its molecular bases, Br. J. Biomed. Sci. 54 (1) (1997) 16–37.
[5] J.B. Lowe, The blood group-specific human glycosyltransferases, Baillieres Clin Haematol 6 (2) (1993) 465–492.
[6] L. Fagerberg, B.M. Hallstrom, P. Oksvold, C. Kampf, D. Djureinovic, J. Odeberg, M. Habuka, S. Tahmasebpoor, A. Danielsson, K. Edlund, A. Asplund, E. Sjostedt, E. Lundberg, C.A. Szigyarto, M. Skogs, J.O. Takanen, H. Berling, H. Tegel, J. Mulder, P. Nilsson, J.M. Schwenk, C. Lindskog, F. Danielsson, A. Mardinoglu, A. Sivertsson, K. von Feilitzen, M. Forsberg, M. Zwahlen, I. Olsson, S. Navani, M. Huss, J. Nielsen, F. Ponten, M. Uhlen, Analysis of the human tissue-specific expression by genome-wide integration of transcriptomics and antibody-based proteomics, Mol. Cell. Proteomics 13 (2) (2014) 397–406.
[7] J.M. Pickard, C.F. Maurice, M.A. Kinnebrew, M.C. Abt, D. Schenten, T. V. Golovkina, S.R. Bogatyrev, R.F. Ismagilov, E.G. Pamer, P.J. Turnbaugh, A. V. Chervonsky, Rapid fucosylation of intestinal epithelium sustains host-commensal symbiosis in sickness, Nature 514 (7524) (2014) 638–+.
[8] P.C. Kashyap, A. Marcobal, L.K. Ursell, S.A. Smits, E.D. Sonnenburg, E.K. Costello, S.K. Higginbottom, S.E. Domino, S.P. Holmes, D.A. Relman, R. Knight, J.I. Gordon, J.L. Sonnenburg, Genetically dictated change in host mucus carbohydrate landscape exerts a diet-dependent effect on the gut microbiota, Proc. Natl. Acad. Sci. U. S. A. 110 (42) (2013) 17059–17064.
[9] T.A. Pham, S. Clare, D. Goulding, J.M. Arasteh, M.D. Stares, H.P. Browne, J. A. Keane, A.J. Page, N. Kumasaka, L. Kane, L. Mottram, K. Harcourt, C. Hale, M. J. Arends, D.J. Gaffney, G. Dougan, T.D. Lawley, Epithelial IL-22RA1-mediated fucosylation promotes intestinal colonization resistance to an opportunistic pathogen, Cell Host Microbe 16 (4) (2014) 504–516.
[10] Y. Goto, T. Obata, J. Kunisawa, S. Sato, Ivanov II, A. Lamichhane, N. Takeyama, M. Kamioka, M. Sakamoto, T. Matsuki, H. Setoyama, A. Imaoka, S. Uematsu, S. Akira, S.E. Domino, P. Kulig, B. Becher, J.C. Renauld, C. Sasakawa, Y. Umesaki, Y. Benno, H. Kiyono, Innate lymphoid cells regulate intestinal epithelial cell glycosylation, Science 345 (6202) (2014) 1254009.
[11] A. Suwandi, A. Galeev, R. Riedel, S. Sharma, K. Seeger, T. Sterzenbach, L. García Pastor, E. Boyle, O. Gal-Mor, M. Hensel, J. Casadesús, J. Baines, G. Grassl, Std fimbriae-fucose interaction increases Salmonella-induced intestinal inflammation and prolongs colonization, PLoS Pathog. 15 (7) (2019).
[12] D. Chessa, M. Winter, M. Jakomin, A. Bäumler, Salmonella enterica serotype Typhimurium Std fimbriae bind terminal alpha(1,2)fucose residues in the cecal mucosa, Mol. Microbiol. 71 (4) (2009).
[13] E.A. Hurd, S.E. Domino, Increased susceptibility of secretor factor gene Fut2-null mice to experimental vaginal candidiasis, Infect. Immun. 72 (7) (2004) 4279–4281.
[14] A. Magalhaes, Y. Rossez, C. Robbe-Masselot, E. Maes, J. Gomes, A. Shevtsova, J. Bugaytsova, T. Boren, C.A. Reis, Muc5ac gastric mucin glycosylation is shaped by FUT2 activity and functionally impacts Helicobacter pylori binding, Sci. Rep. 6 (2016) 25575.
[15] E. Kindberg, B. Akerlind, C. Johnsen, J.D. Knudsen, O. Heltberg, G. Larson, B. Bottiger, L. Svensson, Host genetic resistance to symptomatic norovirus (GGII.4) infections in Denmark, J. Clin. Microbiol. 45 (8) (2007) 2720–2722.
[16] J. Rodriguez-Diaz, I. Garcia-Mantrana, S. Vila-Vicent, R. Gozalbo-Rovira, J. Buesa, V. Monedero, M.C. Collado, Relevance of secretor status genotype and microbiota composition in susceptibility to rotavirus and norovirus infections in humans, Sci. Rep. 7 (2017) 45559.
[17] L. Lindesmith, C. Moe, S. Marionneau, N. Ruvoen, X. Jiang, L. Lindblad, P. Stewart, J. LePendu, R. Baric, Human susceptibility and resistance to Norwalk virus infection, Nat. Med. 9 (5) (2003) 548–553.
[18] F.U. Weiss, C. Schurmann, A. Guenther, F. Ernst, A. Teumer, J. Mayerle, P. Simon, H. Volzke, D. Radke, A. Greinacher, J.P. Kuehn, M. Zenker, U. Volker, G. Homuth, M.M. Lerch, Fucosyltransferase 2 (FUT2) non-secretor status and blood group B are associated with elevated serum lipase activity in asymptomatic subjects, and an increased risk for chronic pancreatitis: a genetic association study, Gut 64 (4) (2015) 646–656.
[19] C. Rupp, K. Friedrich, T. Folseraas, A. Wannhoff, K.A. Bode, K.H. Weiss, P. Schirmacher, P. Sauer, W. Stremmel, D.N. Gotthardt, Fut2 genotype is a risk factor for dominant stenosis and biliary candida infections in primary sclerosing cholangitis, Aliment. Pharmacol. Ther. 39 (8) (2014) 873–882.
[20] D.J. Smyth, J.D. Cooper, J.M. Howson, P. Clarke, K. Downes, T. Mistry, H. Stevens, N.M. Walker, J.A. Todd, FUT2 nonsecretor status links type 1 diabetes susceptibility and resistance to infection, Diabetes 60 (11) (2011) 3081–3084.
[21] D.P. McGovern, M.R. Jones, K.D. Taylor, K. Marciante, X. Yan, M. Dubinsky, A. Ippoliti, E. Vasiliauskas, D. Berel, C. Derkowski, D. Dutridge, P. Fleshner, D. Q. Shih, G. Melmed, E. Mengesha, L. King, S. Pressman, T. Haritunians, X. Guo, S. R. Targan, J.I. Rotter, Fucosyltransferase 2 (FUT2) non-secretor status is associated with Crohn's disease, Hum. Mol. Genet. 19 (17) (2010) 3468–3476.
[22] A. Franke, D.P. McGovern, J.C. Barrett, K. Wang, G.L. Radford-Smith, T. Ahmad, C. W. Lees, T. Balschun, J. Lee, R. Roberts, C.A. Anderson, J.C. Bis, S. Bumpstead, D. Ellinghaus, E.M. Festen, M. Georges, T. Green, T. Haritunians, L. Jostins, A. Latiano, C.G. Mathew, G.W. Montgomery, N.J. Prescott, S. Raychaudhuri, J. I. Rotter, P. Schumm, Y. Sharma, L.A. Simms, K.D. Taylor, D. Whiteman,

C. Wijmenga, R.N. Baldassano, M. Barclay, T.M. Bayless, S. Brand, C. Buning, A. Cohen, J.F. Colombel, M. Cottone, L. Stronati, T. Denson, M. De Vos, R. D'Inca, M. Dubinsky, C. Edwards, T. Florin, D. Franchimont, R. Gearry, J. Glas, A. Van Gossum, S.L. Guthery, J. Halfvarson, H.W. Verspaget, J.P. Hugot, A. Karban, D. Laukens, I. Lawrance, M. Lemann, A. Levine, C. Libioulle, E. Louis, C. Mowat, W. Newman, J. Panes, A. Phillips, D.D. Proctor, M. Regueiro, R. Russell, P. Rutgeerts, J. Sanderson, M. Sans, F. Seibold, A.H. Steinhart, P.C. Stokkers, L. Torkvist, G. Kullak-Ublick, D. Wilson, T. Walters, S.R. Targan, S.R. Brant, J. D. Rioux, M. D'Amato, R.K. Weersma, S. Kugathasan, A.M. Griffiths, J. C. Mansfield, S. Vermeire, R.H. Duerr, M.S. Silverberg, J. Satsangi, S. Schreiber, J. H. Cho, V. Annese, H. Hakonarson, M.J. Daly, M. Parkes, Genome-wide meta-analysis increases to 71 the number of confirmed Crohn's disease susceptibility loci, Nat. Genet. 42 (12) (2010) 1118–1125.

[23] E. Meijerink, S. Neuenschwander, R. Fries, A. Dinter, H. Bertschinger, G. Stranzinger, P. Vögeli, A DNA polymorphism influencing alpha(1,2) fucosyltransferase activity of the pig FUT1 enzyme determines susceptibility of small intestinal epithelium to Escherichia coli F18 adhesion, Immunogenetics 52 (1–2) (2000).

[24] Y. Urata, W. Saiki, Y. Tsukamoto, H. Sago, H. Hibi, T. Okajima, H. Takeuchi, Xylosyl extension of O-glucose glycans on the extracellular domain of NOTCH1 and NOTCH2 regulates notch cell surface trafficking, Cells 9 (5) (2020).

[25] U.K. Laemmli, Cleavage of structural proteins during the assembly of the head of bacteriophage T4, Nature 227 (5259) (1970) 680–685.

[26] S. Alam, Y. Tsukamoto, M. Ogawa, Y. Senoo, K. Ikeda, Y. Tashima, H. Takeuchi, T. Okajima, N-Glycans on EGF domain-specific O-GlcNAc transferase (EOGT) facilitate EOGT maturation and peripheral endoplasmic reticulum localization, J. Biol. Chem. 295 (25) (2020).

[27] M. Lin, I. Munshi, A. Ouellette, The defensin-related murine CRS1C gene: expression in Paneth cells and linkage to Defcr, the cryptdin locus, Genomics 14 (2) (1992).

[28] M. Ismail, E. Stone, M. Panico, S. Lee, Y. Luu, K. Ramirez, S. Ho, M. Fukuda, J. Marth, S. Haslam, A. Dell, High-sensitivity O-glycomic analysis of mice deficient in core 2 {beta}1,6-N-acetylglucosaminyltransferases, Glycobiology 21 (1) (2011).

[29] L. Bry, P. Falk, T. Midtvedt, J. Gordon, A model of host-microbial interactions in an open mammalian ecosystem, Science 273 (5280) (1996).

[30] H. Cash, C. Whitham, C. Behrendt, L. Hooper, Symbiotic bacteria direct expression of an intestinal bactericidal lectin, Science 313 (5790) (2006).

[31] S.H. White, W.C. Wimley, M.E. Selsted, Structure, function, and membrane integration of defensins, Curr. Opin. Struct. Biol. 5 (4) (1995) 521–527.

[32] T. Ayabe, D.P. Satchell, C.L. Wilson, W.C. Parks, M.E. Selsted, A.J. Ouellette, Secretion of microbicidal alpha-defensins by intestinal Paneth cells in response to bacteria, Nat. Immunol. 1 (2) (2000) 113–118.

[33] Y. Shirafuji, H. Tanabe, D. Satchell, A. Henschen-Edman, C. Wilson, A. Ouellette, Structural determinants of procryptdin recognition and cleavage by matrix metalloproteinase-7, J. Biol. Chem. 278 (10) (2003).

[34] K. Masuda, N. Sakai, K. Nakamura, S. Yoshioka, T. Ayabe, Bactericidal activity of mouse α-defensin cryptdin-4 predominantly affects noncommensal bacteria, Journal of innate immunity 3 (3) (2011).

[35] N. Salzman, K. Hung, D. Haribhai, H. Chu, J. Karlsson-Sjöberg, E. Amir, P. Teggatz, M. Barman, M. Hayward, D. Eastwood, M. Stoel, Y. Zhou, E. Sodergren, G. Weinstock, C. Bevins, C. Williams, N. Bos, Enteric defensins are essential regulators of intestinal microbial ecology, Nat. Immunol. 11 (1) (2010).

[36] M.E. Selsted, A.J. Ouellette, Mammalian defensins in the antimicrobial immune response, Nat. Immunol. 6 (6) (2005) 551–557.

[37] K.M. Huttner, M.E. Selsted, A.J. Ouellette, Structure and diversity of the murine cryptdin gene family, Genomics 19 (3) (1994) 448–453.

[38] M. Shanahan, H. Tanabe, A. Ouellette, Strain-specific polymorphisms in Paneth cell α-defensins of C57bl/6 mice and evidence of vestigial myeloid α-defensin pseudogenes, Infect. Immun. 79 (1) (2011).

[39] A.J. Ouellette, J.C. Lualdi, A novel mouse gene family coding for cationic, cysteine-rich peptides. Regulation in small intestine and cells of myeloid origin, J. Biol. Chem. 265 (17) (1990) 9831–9837.

[40] M. Hornef, K. Pütsep, J. Karlsson, E. Refai, M. Andersson, Increased diversity of intestinal antimicrobial peptides by covalent dimer formation, Nat. Immunol. 5 (8) (2004).